

Bayesian estimation of climate sensitivity based on a simple climate model fitted to observations of hemispheric temperatures and global ocean heat content

Magne Aldrin^{a,b*}, Marit Holden^a, Peter Guttorp^{a,c}, Ragnhild Bieltvedt Skeie^d, Gunnar Myhre^d and Terje Koren Berntsen^{d,e}

Predictions of climate change are uncertain mainly because of uncertainties in the emissions of greenhouse gases and how sensitive the climate is to changes in the abundance of the atmospheric constituents. The equilibrium climate sensitivity is defined as the temperature increase because of a doubling of the CO₂ concentration in the atmosphere when the climate reaches a new steady state. CO₂ is only one out of the several external factors that affect the global temperature, called radiative forcing mechanisms as a collective term. In this paper, we present a model framework for estimating the climate sensitivity. The core of the model is a simple, deterministic climate model based on elementary physical laws such as energy balance. It models yearly hemispheric surface temperature and global ocean heat content as a function of historical radiative forcing. This deterministic model is combined with an empirical, stochastic model and fitted to observations on global temperature and ocean heat content, conditioned on estimates of historical radiative forcing. We use a Bayesian framework, with informative priors on a subset of the parameters and flat priors on the climate sensitivity and the remaining parameters. The model is estimated by Markov Chain Monte Carlo techniques. Copyright © 2012 John Wiley & Sons, Ltd.

Keywords: climate change; global warming; radiative forcing; combining computer models and stochastic models; Markov Chain Monte Carlo

1. INTRODUCTION

A key question in the climate change literature is as follows: How does the earth's global temperature depend on the concentration of CO₂ and other greenhouse gases in the atmosphere? This dependency is often quantified by the climate sensitivity, which includes the climate feedbacks in the earth atmosphere system. The climate sensitivity is defined as the equilibrium temperature increase because of a doubling of CO₂ concentration in the atmosphere. However, CO₂ is only one of the several external factors, or radiative forcing mechanisms (Forster *et al.*, 2007), that affect the global temperature. Radiative forcing is composed of the effect of several components, including the concentration of greenhouse gases, aerosols, variations in solar radiation and particles from volcanic eruptions. The global temperature depends on the radiative forcing, and the climate sensitivity is a measure of the strength of this dependency.

The dependency between global temperature and radiative forcing is highly complex and is yet not fully understood (Knutti and Hegerl, 2008; Roe and Baker, 2007; Stainforth *et al.*, 2005). The most detailed and complex climate models, the so called Atmospheric Ocean General Circulation Models (AOGCMs), involve thousands of parameters and are highly computer intensive. Therefore, both from a statistical and a computational point of view, simpler climate models are needed to complement the AOGCMs. Climate models of medium complexity are simpler but rather complex. Another alternative is to use an approximation to the complex or medium complex model, a so-called emulator, where the climate model is approximated by a Gaussian process (e.g. Sansó and Forest, 2009; Drignei *et al.*, 2008), and finally, there are the so-called simple climate models, which are based on elementary physical laws such as energy balance but have a limited number of parameters and only take a few seconds to run (for one set of input values).

* Correspondence to: Magne Aldrin, Norwegian Computing Center, P.O. Box 114 Blindern, N-0314, Oslo, Norway. E-mail: magne.aldrin@nr.no

a Norwegian Computing Center, Norway

b Department of Mathematics, University of Oslo, Oslo, Norway

c Department of Statistics, University of Washington, WA, U.S.A.

d Center for International Climate and Environmental Research - Oslo, Oslo, Norway

e Department of Geosciences, University of Oslo, Oslo, Norway

Several estimates of the climate sensitivity have been presented in recent years. Some of these are based on temperature reconstructions several centuries or millenniums back in time (e.g. Hegerl *et al.*, 2006; Hansen and Sato, 2011), whereas others are based on observed temperatures from the last 150 years or so, for example, Gregory *et al.* (2002) and Forest *et al.* (2006) from the subject-specific literature and Sansó and Forest (2009), Drignei *et al.* (2008) and Tomassini *et al.* (2009) from the statistical literature. In addition, estimates of the climate sensitivity are provided by the AOGCMs (Intergovernmental Panel on Climate Change (IPCC), 2007; Soden and Held, 2006; Stainforth *et al.*, 2005).

In this paper, we present a model framework for estimating the climate sensitivity on the basis of temperature observations. We adopt a very simplistic view of the earth and assume that the “true” global state of the earth in a year consists of three states, namely, (i) the (average) temperature of the northern hemisphere; (ii) the temperature of the southern hemisphere; and (iii) the ocean heat content. The core of the model is a simple, deterministic climate model based on elementary physical laws such as energy balance. It models yearly surface temperature, averaged separately over the northern and southern hemispheres, and ocean heat content as a function of historical radiative forcings. This deterministic model is combined with an empirical, stochastic model and fitted to observations on temperature and ocean heat content, conditioned on estimates of historical radiative forcings. The climate sensitivity is an explicit parameter in the climate model we use, in contrast to more complex climate models where the climate sensitivity is only implicitly defined.

The model is fitted to observational estimates of hemispheric temperatures since 1850, ocean heat content since 1955 and model estimates of radiative forcings since 1750 until 2007. We use a Bayesian framework, with informative priors on a subset of the parameters and flat priors on the climate sensitivity and the remaining parameters. The model is estimated by Markov Chain Monte Carlo (MCMC) techniques.

The data used are described in Section 2, whereas the hierarchical model is contained in Section 3. Results are given in Section 4 and concluding remarks in Section 5. Additional technical details and a comparison with other methods are provided in the electronic Supplementary Material online.[†]

2. DATA

Our response data are estimates of global surface temperature, divided into the northern and southern hemispheres, and in addition, the ocean heat content. Explanatory variables are estimates of radiative forcings and observations of the southern oscillation index (SOI). The last year in all types of data is 2007. Data available from electronic sources were downloaded in May 2010.

2.1. Hemispheric temperatures

The temperatures we will consider are the yearly combined land and sea surface temperatures, averaged separately over the northern and southern hemispheres.

At least three scientific groups produce estimates of these hemispheric temperatures on a routinely basis: the University of East Anglia and the Hadley Centre (HadCRUT3), the Goddard Institute for Space Studies (GISS) and the National Climatic Data Center (NCDC) (Table 1). The three pairs of series are more or less based on the same measurement stations around the world, in total between 4000 and 7000 stations, but the procedures for computing hemispheric averages from the data differ. Each temperature series is given as anomalies from a reference period where the average is approximately zero. For the HadCRUT3 and NCDC data, the annual temperature estimates were accompanied by corresponding standard errors. For the GISS data, standard errors have not been reported, but Hansen *et al.* (2010) indicated that the standard errors of the global temperature series could be around 0.1°C until 1900, around 0.075°C between 1900 and 1950 and around 0.04°C thereafter. However, we need standard errors per hemisphere in our analysis, and it is also reasonable to assume that the standard errors change gradually. For simplicity, we therefore assume that the GISS annual standard errors are proportional to the (yearly) average of the HadCRUT3 and NCDC standard errors, which is roughly consistent with what Hansen *et al.* (2010) indicated.

The three pairs of temperature series are shown in the two upper panels of Figure 1. In this figure, each series is centred to have zero mean in the period 1961–1990, to make the visual comparison easier. The estimates from the three scientific groups are rather similar but not equal. There is no general agreement that one of the three pairs of series is more precise than the others. Therefore, rather than choosing one of them, we use all three simultaneously.

The corresponding reported standard errors of the temperature estimates are shown in the upper two panels of Figure 2. The standard errors decrease as more measurement stations become available during the 20th century but increase slightly at the end of the data period because of reduced number of stations. We note that the reported HadCRUT3 and NCDC standard errors for the southern hemisphere differ notably the last 50 years.

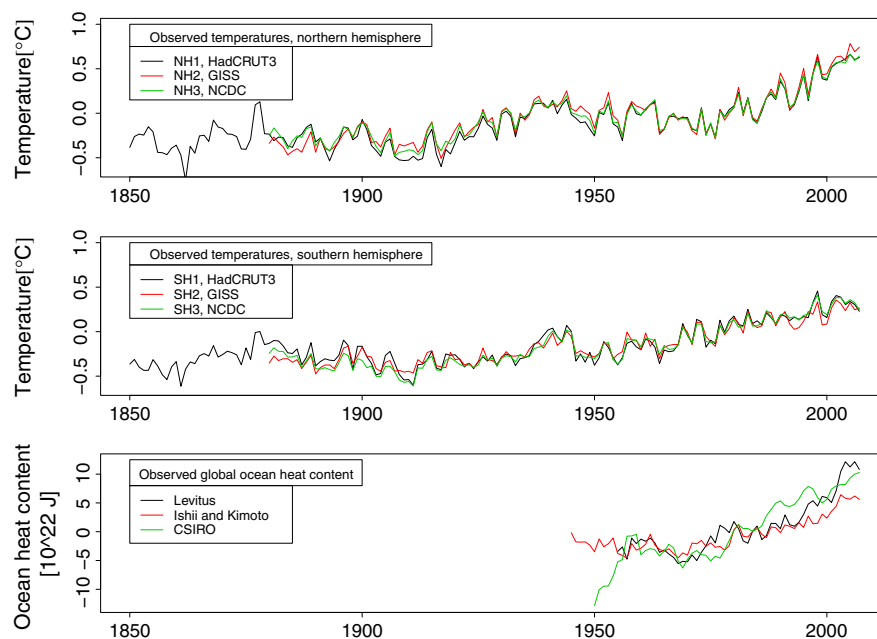
The three pairs of estimated temperature series can also be used to evaluate if their estimation errors or observational errors are autocorrelated. Assuming additive noise, each series can be decomposed as “the true temperature” + error. The difference of two temperature series (e.g. HadCRUT3 and GISS) at the same hemisphere is then the same as the difference between their errors. The autocorrelations at lag one are positive and between 0.5 and 0.7 for all six temperature differences, and they have similar autocorrelation structures also at higher lags (see Figure 7 of the Supplementary Material). Therefore, the observational errors for each temperature series are positively correlated in time as well, and it is further reasonable to believe that their autocorrelation structures are similar between the separate error processes.

[†]Supplementary Material is available online, providing additional information on data, methods, Markov Chain Monte Carlo convergence and results as well as comparisons to other methods.

Table 1. Overview of data sources for the temperatures, the ocean heat contents and the southern oscillation index

Name	Data type	Observation period	Reference period	References	Electronic source
HadCRUT3	Temp.	1850–2007	1961–1990	Brohan <i>et al.</i> (2006)	urlHadCRUT3
GISS	Temp.	1880–2007	1951–1980	Hansen <i>et al.</i> (2010)	urlGISS
NCDC	Temp.	1880–2007	1901–2000	Smith and Reynolds (2005) Smith <i>et al.</i> (2008) Banzon <i>et al.</i> (2010)	urlNCDC
Levitus	OHC	1955–2007	1955–2006	Levitus <i>et al.</i> (2009)	urlNODC
Ishii/Kimoto	OHC	1945–2007	1960–1990	Ishii and Kimoto (2009)	Personal comm. with M. Ishii 5 October 2011
CSIRO	OHC	1950–2007	1960–1990	Church <i>et al.</i> (2011) Domingues <i>et al.</i> (2008)	urlCSIRO
SOI	SOI	1876–2007	none	Trenberth <i>et al.</i> (2002)	urlSOI

HadCRUT3, University of East Anglia and the Hadley Centre; GISS, Goddard Institute for Space Studies; NCDC, National Climatic Data Center; CSIRO, Commonwealth Scientific and Industrial Research Organisation; SOI, southern oscillation index; Temp., temperature; OHC, ocean heat content.

**Figure 1.** Annual temperature and ocean heat data. HadCRUT3, University of East Anglia and the Hadley Centre; GISS, Goddard Institute for Space Studies; NCDC, National Climatic Data Center; CSIRO, Commonwealth Scientific and Industrial Research Organisation

2.2. Ocean heat content

There are also several estimates of the ocean heat content between 0 and 700 m. We will base most of our analysis on the data from Levitus *et al.* (2009), which are available from 1955, but we will also perform separate analyses with two other data series (Table 1). The annual estimates are shown in the lower panel of Figure 1 and the corresponding standard errors in the lower panel of Figure 2.

In principle, the three ocean heat content series could be used simultaneously in the same way as the temperature data. However, this option is not yet included in our computer program, so we will, in the following, use only one ocean heat content series at a time. Unless otherwise specified, the Levitus *et al.* (2009) ocean heat content data are used.

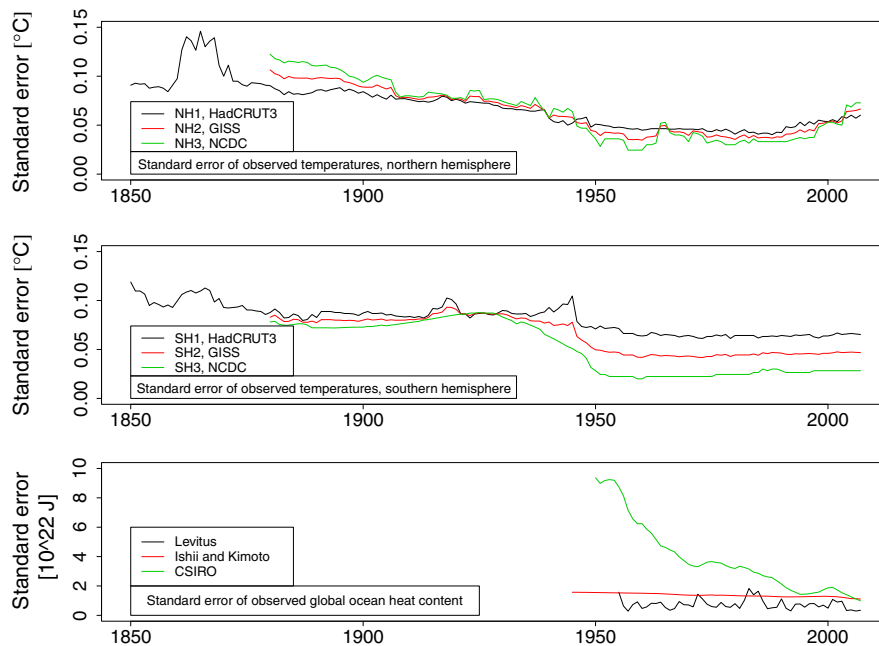


Figure 2. Reported standard errors of annual temperature and ocean heat data. The standard errors for the Goddard Institute for Space Studies (GISS) series are simply computed as the middle of the standard errors for the two other series. HadCRUT3, University of East Anglia and the Hadley Centre; NCDC, National Climatic Data Center; CSIRO, Commonwealth Scientific and Industrial Research Organisation

2.3. Radiative forcings

The data for radiative forcings are not direct observations but rather estimates with specified uncertainties based on (temperature-independent) information from several sources. These estimates are given for each hemisphere and each year from 1750 to 2007. The uncertainty distributions for the radiative forcings will act as prior distributions in our analysis.

The total radiative forcing is the changes over the industrial era of the sum of the contribution from the following nine components: long-lived greenhouse gases (CO₂, CH₄, N₂O and halocarbons), tropospheric ozone, stratospheric ozone, stratospheric H₂O, the direct aerosol effect, the cloud albedo effect (indirect aerosol effect), surface albedo because of land use changes, solar radiation and volcanoes. For each component, except volcanoes, the estimated radiative forcing in 2005 with 90% uncertainty interval is given in Table 2.12 in Chapter 2 of the IPCC report from 2007 (Forster *et al.*, 2007). The time development of each component from 1750 to 2007 is based on various sources (mainly Myhre *et al.*, 2001) but made consistent with the IPCC 2005 estimates. Because radiative forcing is the change in net irradiance relative to 1750, all components are by definition zero in 1750. Therefore, also the standard deviations of the estimated errors of each component are exactly zero in 1750, and further assumed to be consistent with the IPCC uncertainties for 2005 and moreover proportional either to time since 1750 or to the absolute level of the component. The distributions of the estimation errors of each component are assumed to be either normal, truncated (at zero) normal or lognormal (Section 1.1 of the Supplementary Material).

For volcanoes, we use a point estimate, that is, the yearly weighted average of three different published estimates (Gao *et al.*, 2008; Crowley *et al.*, 2003; Ammann *et al.*, 2003). For the uncertainty, we assume the quite conservative factor of 2, that is, a 90% uncertainty interval is $[0.5\hat{\mu}, 2\hat{\mu}]$ when the point estimate is $\hat{\mu}$. Smaller uncertainty intervals have been indicated in Gao *et al.* (2008) and Sato *et al.* (1993). In Gao *et al.* (2008), the authors concluded that their “uncertainty range is much smaller than the factor of 2 uncertainty estimate in the earlier studies.”

The uncertainty distributions for four of the components are shown in Figure 3. Because radiative forcing is the change in net irradiance relative to 1750, the uncertainties increase gradually by time (even if the estimates of the *absolute* irradiance levels are more precise today). The radiative forcing because of long-lived greenhouse gases (upper panels) has increased significantly since 1750. The solar radiation (second row of the panels) shows a clearly cyclical pattern (the 11-year cycle) with a rather high uncertainty upwards. The volcanoes (third row of the panels) can give a very large negative radiative forcing in shorter periods, but most of the time their contributions are close to zero. Finally, the radiative forcing because of direct aerosols (lower panels) has a large uncertainty, and even its sign is uncertain because it is a sum of subcomponents with both negative and positive forcings. Furthermore, the effect of this component is much larger in the northern hemisphere than in the southern hemisphere.

The total radiative forcing for each hemisphere is the sum of the contribution from each of the nine components. The global radiative forcing is further the average of the two hemispheric forcings and is shown as the prior in Figure 4. There is indication of an increasing radiative forcing, but the uncertainty is large because of components with negative forcings and large uncertainties, mainly the aerosol effects. In the calculations of the radiative forcing, the spectral overlap between some of the greenhouse gases (e.g. between CH₄, N₂O) has been taken into account. Using a global climate model, Meehl *et al.* (2004) demonstrated that when responses from the individual forcings are added and their sum is compared with a simulation where they are all included together, there is a close correspondence.

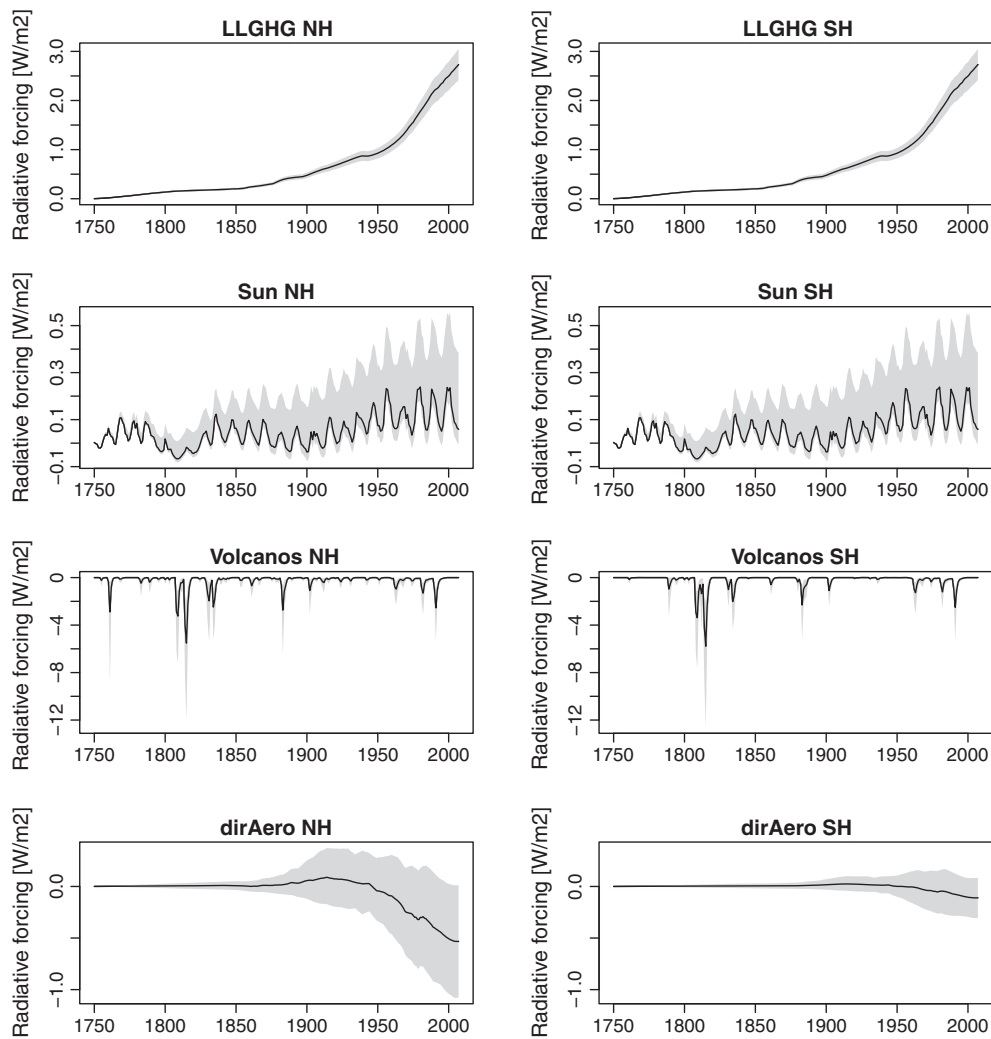


Figure 3. Priors for four components of radiative forcing, for the northern (NH; left panels) and southern (SH; right panels) hemispheres. LLGHG, long-lived greenhouse gases; dirAero, direct aerosols

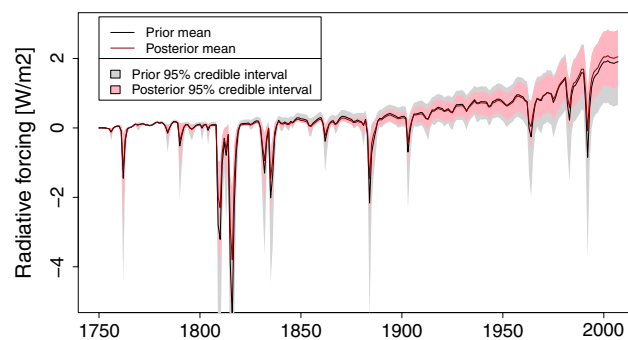


Figure 4. Posterior and prior for the global radiative forcing

More information on the estimates of the radiative forcings and their uncertainties is found in Section 1.1 of the Supplementary Material.

2.4. Southern oscillation index

The global mean surface temperature is influenced by natural variability. The most important fluctuation is the El Niño-Southern Oscillation (Trenberth *et al.*, 2002) (Table 1). During El Niño episodes, there is a warming of the surface of the tropical eastern Pacific Ocean

and hence an influence on the hemispheric temperatures. The SOI is calculated from the monthly fluctuations in the air pressure difference between Tahiti and Darwin, Australia. Sustained negative values of the SOI indicate El Niño episodes and are therefore associated with the hemispheric temperatures. We have aggregated the monthly SOI values to yearly averages, but because the SOI precedes the temperature, the SOI for year t is averaged over the last 6 months of year $t - 1$ and the first 6 months of year t . This choice is based on a rough preliminary analysis of the correlation between the yearly temperatures and the lagged yearly SOI. The SOI values are available from 1876, but because of the lagging, the first year in our aggregated series is 1877.

3. METHODS

We adopt a rather simplistic view of the world and define the “true” global state of the earth in year t as a three-dimensional vector with three elements: (i) the true temperature of the northern hemisphere; (ii) the true temperature of the southern hemisphere, and (iii) the true ocean heat content. We denote this true state vector by \mathbf{g}_t .

We have corresponding observations (or rather estimates based on observations), denoted by the vector \mathbf{y}_t . Because we have three pairs of temperature series, \mathbf{y}_t has dimension seven, where the first three elements are the HadCRUT3, GISS and NCDC temperatures of the northern hemisphere, respectively, the next three elements are the corresponding temperatures of the southern hemisphere and the last element is the observed (or estimated) ocean heat content. Furthermore, the observations are accompanied with a corresponding vector \mathbf{s}_t of reported standard errors.

Our full model consists of a process model for the true process \mathbf{g}_t and a data model for the observations \mathbf{y}_t . The core of the process model is a simple climate model based on physical laws. The climate model is purely deterministic, often also termed a computer model. Therefore, in the process model, it is combined with a stochastic term.

3.1. The simple climate model

The simple climate model is an energy-balance climate/upwelling diffusion ocean (EBC/UDO) model developed by Schlesinger *et al.* (1992). Olivie and Stuber (2010) showed that the simple climate model with optimized parameter sets is able to reproduce the complex response of AOGCMs. The simple climate model has been applied in a number of studies to simulate the temporal response of the climate system to various emission scenarios (e.g. Skeie *et al.*, 2009). With prescribed values for climate sensitivity and other model parameters, as well as for historical radiative forcings, the model calculates yearly changes in hemispheric mean temperatures and global ocean heat content. The equilibrium climate sensitivity is a prescribed parameter in the model that represents the feedbacks of the climate system. Although the climate system is presently not in equilibrium because of the long timescales needed for transport of heat to the deep ocean, the equilibrium climate sensitivity can still be estimated on the basis of the transient response of the model. The model is constructed so that the temperature increase will be equal to the climate sensitivity when the model is run to equilibrium with a forcing corresponding to a doubling of the CO₂ concentration.

Radiative forcings are input to the system, and the simple climate model calculations are based on formulations for the exchange of energy between the atmosphere and the water surface and further down to the deep ocean as well as between the two hemispheres in the ocean (see Figure 5). The surface layer of the ocean is set to a thickness around 75 m (input to the model), whereas the underlying part is split into 40 layers, each of thickness 100 m. The transportation of cold water directly to the deep oceans in the polar regions is accounted for. For further details of this model, see Schlesinger *et al.* (1992). The EBC/UDO model has a structure similar to the models used by IPCC in the Second Assessment Report (Houghton *et al.*, 1996) as described in Houghton *et al.* (1997). EBC/UDO models do not resolve internal natural variability in the climate system; they only calculate temperature change because of external forcing.

The output from the climate model is a three-dimensional vector, denoted by \mathbf{m}_t , with (model values of) the temperatures of the northern and southern hemispheres and the global ocean heat content in year t . It is a function of the yearly historical radiative forcing $\mathbf{x}_{1750:t}$ from 1750 to year t , divided into the two hemispheres. The model output is further a function of the climate sensitivity S , which is the parameter of interest, and a six-dimensional vector θ of other model parameters listed in Table 2. Here, for instance, the mixed layer is the uppermost layer of the ocean where heat is exchanged with the atmosphere. In addition, we assume that the atmospheric heat exchange between the two hemispheres is negligible, that is, the corresponding parameter is set to zero. A more detailed description of the model parameters are found in Section 2.1 of the Supplementary Material. We write the output of and input to the model in full as $\mathbf{m}_t(\mathbf{x}_{1750:t}, S, \theta)$.

3.2. The process model

The process model describing the true state of the earth \mathbf{g}_t in year t is a combined deterministic and stochastic model given by

$$\mathbf{g}_t = \mathbf{m}_t(\mathbf{x}_{1750:t}, S, \theta) + \beta_1 \cdot e_t + \mathbf{n}_t^m \tag{1}$$

Here, $\mathbf{x}_{1750:t}$, S and θ are the true, but unknown, input values to the climate model. Furthermore, the scalar e_t is the SOI, and the regression coefficient β_1 is a three-dimensional vector expressing the effect of the SOI. The two first elements of β_1 are the effects on the temperatures of the northern and southern hemispheres, respectively. The third element, corresponding to the effect on the ocean heat content, is set to zero because we expect that there is no relationship between the SOI and the ocean heat content. The term $\beta_1 \cdot e_t$ can be interpreted as a refinement of the climate model. Finally, \mathbf{n}_t^m is a three-dimensional vector of model errors.

We assume that the model errors follow a vector autoregressive process of order one, that is,

$$\mathbf{n}_t^m = \Phi^m \mathbf{n}_{t-1}^m + \boldsymbol{\varepsilon}_t^m \tag{2}$$

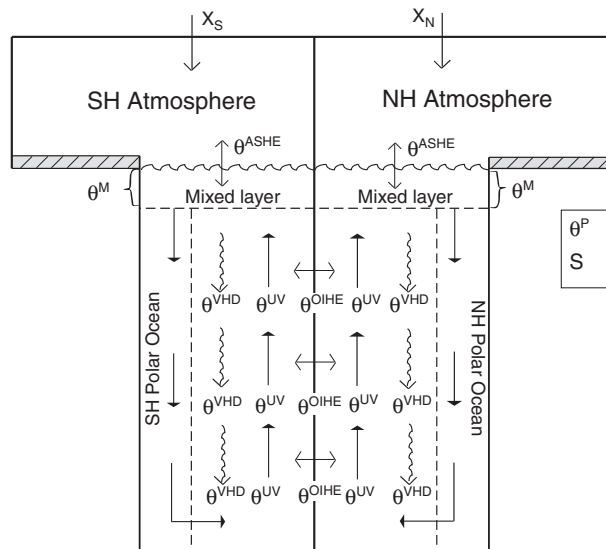


Figure 5. The climate model. SH, southern hemisphere; NH, northern hemisphere

Table 2. Climate model parameters, with prior distributions and prior and posterior means and 95% credible intervals from the main analysis

Notation	Name	Unit	Prior distribution	Prior mean and 95% credible interval	Posterior mean and 95% credible interval
S	Climate sensitivity	K	Uniform($10^{-4}, 20$)	10.0 (0.50,19.5)	1.98 (1.07,4.28)
θ^M	Mixed layer depth	m	Uniform(25,125)	75.0 (27.5,122.5)	74.6 (28.8,121.5)
θ^P	Polar parameter		Uniform(0.161,0.569)	0.37 (0.17,0.56)	0.37 (0.17,0.56)
θ^{ASHE}	Air-sea heat exchange parameter	$W/m^2 K$	Uniform(5,25)	15.0 (5.5,24.5)	12.8 (5.2,24.1)
θ^{OIHE}	Oceanic interhemispheric heat exchange coefficient	$W/m^2 K$	Uniform(0,7)	3.50 (0.18,6.83)	4.01 (0.39,6.87)
θ^{UV}	Upwelling velocity	$m/year$	Uniform(0.55,2.55)	1.55 (0.60,2.50)	1.47 (0.59,2.49)
θ^{VHD}	Vertical heat diffusivity	cm^2/sec	Defined by $\theta^{VHD} = H \cdot \theta^{UV} / 3153.6$ where $H \sim$ Uniform(400,1000) (in m)	0.34 (0.11,0.69)	0.30 (0.12,0.57)

where Φ^m is a 3×3 diagonal matrix and the noise term ϵ_t^m is a three-dimensional vector assumed to be normally distributed with zero expectation and covariance matrix Σ^m and uncorrelated in time. This model allows the three elements of \mathbf{n}_t^m to be correlated with each other within the same year and over time.

Observations indicate that there may be significant multidecadal internal variability in the climate system (Trenberth *et al.*, 2007; Hegerl *et al.*, 2007). It has been suggested to be a source of such variability with a period of about 50 years and a potential peak-to-peak variability in northern hemisphere decadal mean temperatures of $0.2^\circ C$ (Knight *et al.*, 2005; Semenov *et al.*, 2010). The role of the model error \mathbf{n}_t^m is to account for such internal variability and other deficiencies of our simple climate model.

3.3. The data model

The data model or the observation model is the model for the observations \mathbf{y}_t conditioned on the state \mathbf{g}_t of the process and is here given by

$$\mathbf{y}_t = \mathbf{A}\mathbf{g}_t + \beta_0 + \mathbf{n}_t^o \tag{3}$$

Here, \mathbf{A} is a 7×3 matrix with value 1 on elements (1,1), (2,1), (3,1), (4,2), (5,2), (6,2) and (7,3) and 0 elsewhere, just copying the northern and southern temperatures three times and the ocean heat content once to compare the model output with observations. Furthermore, β_0 is a seven-dimensional vector of intercepts, which is included because the measurements and the output of the computer model are given

relative to the mean of different reference periods (see Section 2.3 of the Supplementary Material). Finally, \mathbf{n}_t^o is a seven-dimensional vector of observational (measurement) errors.

We assume that the observational errors follow a scaled vector autoregressive process of order one, where the scaling factor is given by the vector of standard errors \mathbf{s}_t . To be more specific,

$$\mathbf{n}_t^o = \text{diag}(\mathbf{s}_t)\mathbf{n}_t^{*o} \tag{4}$$

where $\text{diag}(\mathbf{s}_t)$ is a diagonal matrix with \mathbf{s}_t on the diagonal and \mathbf{n}_t^{*o} is an ordinary vector autoregressive process, that is,

$$\mathbf{n}_t^{*o} = \Phi^o \mathbf{n}_{t-1}^{*o} + \boldsymbol{\varepsilon}_t^o \tag{5}$$

where the various symbols have the same meaning as for the model errors but with dimension seven instead of three. To restrict the number of free parameters, the three autoregressive parameters for the northern hemisphere temperature are assumed to be equal and similarly for the southern hemisphere (see the end of Section 2.1 for a motivation).

The standard deviation of the i th element \mathbf{n}_t^{*o} is $s_i^* = \sqrt{\sigma_{ii}^2 / (1 - \phi_{ii}^2)}$, where σ_{ii}^2 is the i th diagonal element of the covariance matrix Σ^o of $\boldsymbol{\varepsilon}_t^o$ and ϕ_{ii} is the i th diagonal element of Φ^o . The corresponding standard deviation of the i th element of the observational error \mathbf{n}_t^o is therefore $s_{ti} \cdot s_i^*$, where s_{ti} is the i th element of the vector of reported standard errors \mathbf{s}_t . This means that s_i^* is a factor that corrects for underestimation or overestimation of the reported standard error s_{ti} and that we take into account only the temporal trend of s_{ti} , not it's magnitude.

3.4. Estimation

The model is estimated on the basis of the observations \mathbf{y}_t from 1850 to 2007, where some elements of \mathbf{y}_t are missing until 1954. We apply a Bayesian approach in the spirit of Kennedy and O'Hagan (2001) on calibration of computer models but without using an emulator to approximate the computer model. Prior distributions are specified for all unknown quantities, see the following text. We use MCMC techniques to sample from the posterior distribution. We have implemented a Metropolis–Hastings sampler where the parameters are updated in blocks. The parameter blocks are updated either by a random-walk update or by using a Gibbs sampler. A random-walk update is used when the prior distribution is normal or uniform, whereas a Gibbs-sampler update is used when the prior is gamma or Wishart. More information on the MCMC algorithm is found in Section 2.4 of the Supplementary Material.

3.5. Priors

We use informative priors for quantities where we have certain knowledge and vague priors for other quantities. The prior distributions are independent of each other if nothing else is indicated.

In particular, for the climate sensitivity S , which is the parameter of interest, we use a rather vague prior but constrained to be non-negative. To be more specific, it is uniform between a very small positive number and 20°C (Table 2). For the other parameters of the climate model, we use informative, uniform priors, independent for each parameter (Table 2). Here, the priors of θ^{UV} and H are independent, but the priors of θ^{UV} and θ^{VHD} are dependent in a physically meaningful way because the latter is given by $\theta^{VHD} = H \cdot \theta^{UV} / 3153.6$ (see details in Section 2.1 of the Supplementary Material).

For the radiative forcings, we treat the temperature-independent estimates and uncertainty distributions presented in Section 2.3 as prior distributions. The estimation errors are independent between components because they are based on independent information, and therefore the priors are independent as well. Within each component, however, the priors are exact dependent (i.e. have correlation one) between the two hemispheres and between different years. Note that independent priors here mean independence in the sense that the random deviations from the curves of yearly expectations are independent between components. The curves of yearly expectations themselves are still similar between some components because many of them are a result of the same industrial development.

The priors of each element of the intercept β_0 and the regression coefficient β_1 are vague, uniform between -10^4 and 10^4 . The autoregressive coefficients on the diagonals of Φ^m and Φ^o are uniform between 0 and 0.9999. For the covariance matrix Σ^m , we use a vague, but structured prior, in that the inverse matrix $(\Sigma^m)^{-1}$ is Wishart (3 degrees of freedom, I_3), where the scale matrix I_3 is the 3×3 identity matrix. Likewise, $(\Sigma^o)^{-1}$ is Wishart (7 degrees of freedom, I_7).

Finally, remember that the SOI e_t was known from 1877 but unknown between 1850 and 1876. With a preliminary analysis of the observed values, we specify an autoregressive model of order two for the SOI, with flat priors restricted to ensure stationarity and invertibility for the two autoregressive coefficients and a vague gamma prior for the variance. In addition to the priors described earlier, we need priors for a few initialization values in the start or end of the time series. More details on all priors are found in Sections 1.2 and 2 of the Supplementary Material.

4. RESULTS

In this section, we first present the results from the main analysis, on the basis of the data set and methodology described in previous sections. Then, we evaluate the model's ability to capture the main features in a better constrained but more hypothetical world by fitting it to artificial data generated by three AOGCMs where the "true" underlying climate sensitivity is known. Furthermore, we test the model's prediction performance and investigate the sensitivities in the main results to changes in the priors. We also investigate the effect of adding an extra component to the total radiative forcing to account for indirect cloud effects not included in the standard IPCC definition of radiative forcing.

These are fast feedbacks that do not require a change in surface temperatures (Lohmann *et al.*, 2010). Finally, we re-estimate the climate sensitivity by using either only the temperature data or only the ocean heat content data.

In each case, two independent chains are run from the same set of start values, one with 100 million and another with 50 million iterations. The first 6 million iterations of each chain are used for burn in, and the remaining $94 + 44 = 138$ million iterations are used for estimation of the posterior distribution but thinned such that only each 5000th iteration was used. The convergence of the chains were evaluated by visual inspection of the iteration traces for the parameters (see Section 3.1 of the Supplementary Material).

4.1. Main results

Panel (a) of Figure 6 shows the posterior distribution of the climate sensitivity. The posterior mean is 2.0°C (see also Table 2), which is lower than the IPCC estimate from the IPCC Fourth Assessment Report (IPCC, 2007), but this estimate increases if an extra forcing component is added, see the following text. The 95% credible interval (CI) ranges from 1.1°C to 4.3°C, whereas the 90% CI ranges from 1.2°C to 3.5°C. There is a small probability for S being larger than 10°C (posterior estimate 0.001). Annan and Hargreaves (2011) argued against uniform priors for S because the posterior can depend on the upper limit of the prior. However, this happens only when the data support values of S above the prior upper limit, which does not happen in our case. The choice of prior for S is still important, however, and we investigate the sensitivity to the choice of prior in the following text. A measure of relative uncertainty, denoted R90, has been calculated as the width of the 90% CI divided by the posterior mean and is here 1.17. This measure is useful when we later compare the estimation uncertainties on the basis of different assumptions because the absolute uncertainty typically increases with increasing posterior mean.

Even if the posterior distributions are based on 27 600 (after thinning) simulated values of S , the errors because of the Monte Carlo sampling are not necessarily negligible because the simulated values are positively correlated. The Monte Carlo errors have been calculated by a simple block bootstrap procedure (Künsch, 1989), dividing the trace of the simulated values of S into 60 blocks each of length 460 and sampling from these randomly with replacement. The standard errors are around 0.5% for lower limits of both the 90% and 95% CIs, 2% for the posterior mean, 4% for the upper limit of the 90% interval and 7% for the upper limit of the 95% interval.

Figure 7 shows the observed HadCRUT3 temperatures and the ocean heat content, together with the corresponding fitted values based on the posterior mean of $\mathbf{A}[\mathbf{m}_t(\mathbf{x}_{1750:t}, S, \theta) + \beta_1 \cdot e_t] + \beta_0$, that is, with the error terms set to zero. The observed and fitted values for the GISS and NCDC temperatures are similar but not shown here. The fitted values follow the main trends of the observations. Furthermore, some of the shorter fluctuations in the temperature data have been picked up by the model, mainly because of the inclusion of the SOI in the model. This shows that the process model, that is, the physical part of the full model, is able to explain certain aspects of the variations in the data.

Figure 4 shows the posterior and the prior of the global radiative forcing. The posterior mean is close to the prior mean, but the posterior uncertainty is somewhat reduced compared with that of the prior. Remember that the radiative forcing is the change relative to the situation in 1750, and therefore its uncertainty increases by time. We presented the priors of four separate components in Figure 3. For the long-lived greenhouse gases and the direct aerosols, which have a very smooth time profile, the posteriors are almost the same as the priors (these and other posteriors of the single forcing components are shown in Section 3.6 of the Supplementary Material). On the other hand, the solar radiation has a very fluctuating profile, and for this component, the posterior has much less uncertainty than the prior and is concentrated in the lower part of the prior. The forcing because of volcanoes has also a fluctuating pattern over time, and the uncertainty of the posterior is about half of that of the prior.

The posterior mean and CIs of the parameters of the climate model are given in the rightmost column of Table 2. Except for the climate sensitivity, the posterior 95% CIs are only slightly narrower than the corresponding intervals of the uniform priors, indicating that the data contain little information on these parameters.

The posterior summaries of the parameters of the model error process are given in Table 3. The covariance matrix Σ^m is here decomposed as $\Sigma^m = \text{diag}(\sigma^m) \mathbf{C}^m \text{diag}(\sigma^m)$, where σ^m is the vector of standard deviations and \mathbf{C}^m is a correlation matrix. The autocorrelations are clearly different from zero, with posterior means between 0.6 and 0.7. There is a small positive correlation between the air temperature errors for the two hemispheres, but the temperature errors are seemingly uncorrelated with the errors in the ocean heat content.

Likewise, Table 4 shows the estimates of the parameters in the observational error process. Here, the autocorrelations are slightly less than for the model error process. There are positive correlations between the temperature errors within each hemisphere but not between hemispheres. Again, the temperature errors are nearly uncorrelated with the errors in the ocean heat content, at least compared with the large uncertainties.

Table 4 also shows the s_i^* 's, that is, the adjusting factors for the reported standard errors of the temperature and ocean heat content estimates. The main impression is that the reported standard errors for the ocean heat content are roughly correct (s^* close to 1), but they may be overestimated for the HadCRUT3 and NCDC temperature series (s^* 's well below 1). The estimates of the GISS factors are both above 1, indicating that our pre-assumed GISS level between HadCRUT3 and NCDC may be too low.

It is conceptually useful to divide the errors into model errors and observational errors, and some of the results shown earlier (at least the correlations) seem intuitively very reasonable. However, the two error terms may be hard to separate, so one should be careful with too strict an interpretation of each term.

The two non-zero elements of β_1 express the effect of the SOI on the temperatures. Their posterior estimates are $-0.51 \cdot 10^{-3}$ (95% CI $-0.77 \cdot 10^{-3}, -0.26 \cdot 10^{-3}$) and $-0.44 \cdot 10^{-3}$ ($-0.65 \cdot 10^{-3}, -0.22 \cdot 10^{-3}$) for the northern and southern hemispheres, respectively, that is, negative SOI values tend to be associated with hemispheric warming. The two autoregressive parameters in the SOI-process (which was assumed to be AR(2)) are estimated to have the so-called complex roots, which correspond to a pseudo-periodic behaviour of the SOI-process with an average period of 5 years. This is in accordance with general knowledge on the SOI.

The importance of the effect of SOI, the model error and the observational error can be compared by comparing their standard deviations. The standard deviations are 0.05 for the SOI effect at both hemispheres and 0.17, 0.15 and 1.5 for the model errors at the northern and

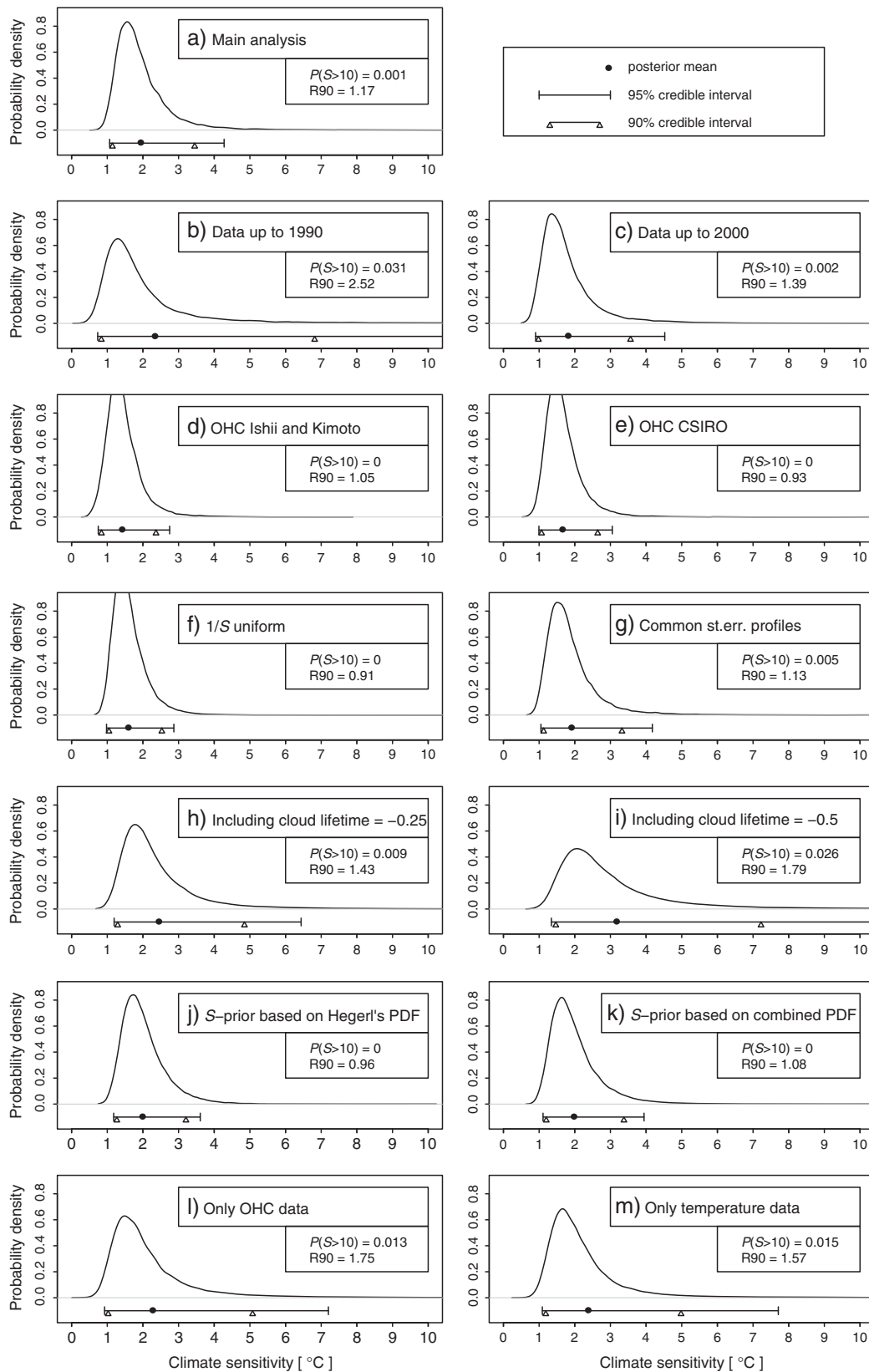


Figure 6. Posterior distributions for the climate sensitivity for the main analysis and several re-analyses. The range of each density function is equal to the range of the simulated values from the Markov Chain Monte Carlo algorithm. The estimated probabilities of S being larger than 10°C and the widths of the relative 90% credible intervals (R90) are given in the lower text box of each panel. PDF, probability density function; CSIRO, Commonwealth Scientific and Industrial Research Organisation; st.err., standard error; OHC, ocean heat content

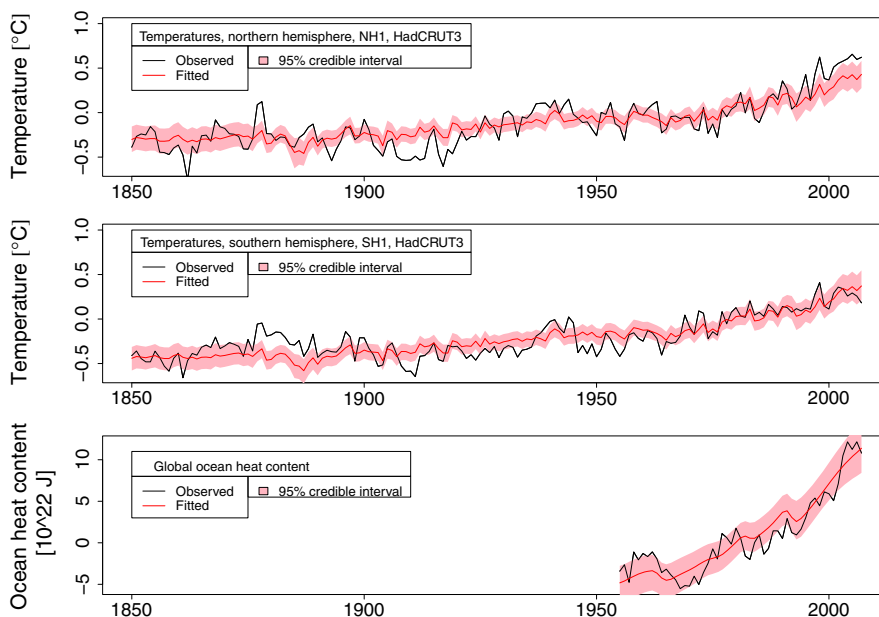


Figure 7. Observed and fitted (posterior mean) values for the University of East Anglia and the Hadley Centre (HadCRUT3) temperature series and the ocean heat content series

Table 3. Estimates (posterior means) with 95% credible intervals for parameters in the model error process

	ϕ^m	σ^m	Correlation matrix C^m		
			Temp. NH	Temp. SH	OHC
Temp. NH	0.65 (0.46,0.84)	0.13 (0.12,0.15)	1		
Temp. SH	0.70 (0.49,0.88)	0.11 (0.10,0.13)	0.2 (0,0.4)	1	
OHC	0.63 (0.23,0.94)	1.18 (0.85,1.54)	0 (-0.2,0.2)	0 (-0.3,0.2)	1

Temp., temperature; NH, northern hemisphere; SH, southern hemisphere; OHC, ocean heat content.

southern hemispheres and the ocean heat content, respectively. Finally, the standard errors for the observational errors are between 0.02 and 0.06 for the six temperatures and 0.7 of the ocean heat content. Thus, the model error is considerably larger than both the observational error and the SOI effect. However, note that the differences between the Levitus series and the two other data series for the ocean heat content (see Figure 1) are many times larger than the estimated standard deviation of 0.7 for the Levitus series, so the real observational error for the ocean heat content may be larger and the model error correspondingly less.

Some additional results are shown in Section 3 of the Supplementary Material.

4.2. Validation on data from Atmospheric Ocean General Circulation Models

Our model is an extreme simplification to the complex phenomenon we attempt to imitate. It is based on a simple climate model with autocorrelated model and observational errors and is unable to simulate modes of natural variability in the climate system and without any state dependency for climate sensitivity. Therefore, to investigate if our model is relevant for the study of the true climate, it is validated on artificial data generated from three different AOGCMs in the Coupled Model Intercomparison Project phase 3 (CMIP3) multimodel data set (urlCMIP3), which has been used for the IPCC Fourth Assessment Report (IPCC, 2007).

The CMIP3 experiments consist of model runs from several AOGCMs, simulating an idealized situation where the CO₂ concentration increases with 1% per year from 1859 to a doubling in 1929, with a subsequent stabilization. This corresponds to the radiative forcing increasing linearly from 0 in 1859 to 3.7 W/m² in 1929 (Figure 8). The simulations end in 2079.

Time series of temperatures for the two hemispheres and the ocean heat content have been generated from each AOGCM. In this ideal example, the implicit “true” climate sensitivity is known for each AOGCM. Note that this is a very different situation from today’s climate, and the simulated climate in this period is not at all related to the real climate in the same period, but it is nevertheless a useful experiment.

Table 4. Estimates (posterior means) with 95% credible intervals for parameters in the observational error process

	s^*	Φ^o	σ^o	Correlation matrix C^o								
				NH1 HadCRUT3	NH2 GISS	NH3 NCDC	SH1 HadCRUT3	SH2 GISS	SH3 NCDC	OHC		
NH1 HadCRUT3	0.65 (0.44,0.92)	0.57 (0.45,0.68)	0.53 (0.36,0.75)	1								
NH2 GISS	1.11 (0.77,1.52)	as above	0.91 (0.64,1.21)	0.3 (-0.2,0.7)	1							
NH3 NCDC	0.61 (0.38,0.93)	as above	0.50 (0.31,0.75)	0.4 (-0.1,0.7)	0.6 (0.1,0.9)	1						
SH1 HadCRUT3	0.82 (0.62,1.07)	0.57 (0.46,0.70)	0.67 (0.52,0.84)	0.2 (-0.2,0.6)	0 (-0.3,0.4)	0.1 (-0.4,0.6)	1					
SH2 GISS	1.16 (0.86,1.52)	as above	0.94 (0.73,1.18)	0 (-0.5,0.5)	0.1 (-0.3,0.4)	0.1 (-0.5,0.6)	0.2 (-0.1,0.5)	1				
SH3 NCDC	0.61 (0.38,0.91)	as above	0.50 (0.32,0.73)	0.1 (-0.4,0.6)	-0.2 (-0.7,0.4)	0 (-0.5,0.6)	0.5 (0.1,0.8)	0.3 (-0.3,0.7)	1			
OHC	1.07 (0.49,2.34)	0.54 (0.05,0.93)	0.77 (0.43,1.27)	0.1 (-0.5,0.7)	0.2 (-0.5,0.7)	0.1 (-0.5,0.7)	0.2 (-0.4,0.7)	0.1 (-0.4,0.6)	0.1 (-0.5,0.6)	1		

NH, northern hemisphere; SH, southern hemisphere; HadCRUT3, University of East Anglia and the Hadley Centre; GISS, Goddard Institute for Space Studies; NCDC, National Climatic Data Center; OHC, ocean heat content.

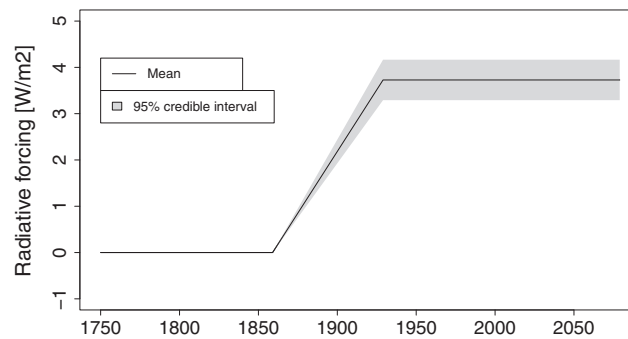


Figure 8. Coupled Model Intercomparison Project phase 3 experiment: Prior for the global radiative forcing

We use the CMIP3 data from the Canadian AOGCM named CGCM3.1(T47) (Scinocca *et al.*, 2008), the GISS-ER (Schmidt *et al.*, 2006) and the IPSL-CM4 (Hourdin *et al.*, 2006), with “true” climate sensitivities of 3.4°C, 2.7°C and 4.4°C, respectively, as reported by the modelling groups (Randall *et al.*, 2007). We extract a training data set from these data, using one AOGCM at a time, estimate our model, including the climate sensitivity, from the training data and predict future temperatures and ocean heat content. The training data set consists of temperature and ocean heat content data from 1860 to 1920. These data are the “true” values. To come closer to the real situation, we simulate observational errors for each of the three pairs of temperature series and the ocean heat content from the fitted models described in Section 4.1 and add them to the “true” values, which gives us three pairs of simulated “observed” temperature series and one simulated “observed” ocean heat content series, with the exception that the standard errors are constant over time and the initial standard errors s_T being 0.05°C for the temperatures and $1 \cdot 10^{22}$ J for the ocean heat content. The radiative forcing of the change in the CO₂ concentrations defined in the CMIP3 experiment was calculated using the relation given in (Ramaswamy *et al.*, 2001). As prior for the radiative forcing, we use a normal distribution with expectation of the “true” forcing, with a 95% CI between –16.5% and 16.5% (Figure 8) and with correlation one between years and between the two hemispheres.

In these experiments, we used wider priors for some of the parameters in the simple climate model, motivated by results reported in Olivie and Stuber (2010) (see Section 3.4 of the Supplementary Material for details). Furthermore, because the SOI was not reported to the CMIP3 database, we here assumed that all SOI values are missing (however, the SOI values could probably have been calculated from other variables that were reported).

Figure 9 shows, for the CGCM3.1(T47) experiment, the “true” temperatures and ocean heat content from 1860 to 2079, the simulated “observed” HadCRUT3 temperature series and ocean heat content in the first training period and their predicted values with uncertainty in the following period up to 2079. Differences between the “true” and the fitted values in the training data period represent both the model errors and the variations because of the SOI (because the SOI values are missing, see earlier text). The differences between the “true” and the predicted values in the prediction periods are also influenced by the estimation errors of the parameters, resulting in a systematic deviation between the two curves. The simulated “observed” GISS and NCDC temperature series are also used for estimation but not shown in the figure. Remember that the climate sensitivity is the equilibrium temperature change because of a doubling of the CO₂ concentration and in Figure 9, this is the asymptote where the temperatures at the two hemispheres will stabilise after many hundred years. The results for the experiments based on the two other AOGCMs are similar (Figures 9 and 10 of the Supplementary Material).

The corresponding estimates of the climate sensitivities are 3.6°C (95% CI 2.5°C, 5.6°C, “true” value 3.4°C), 3.1°C (CI 2.1°C, 5.0°C, “true” value 2.7°C) and 3.3°C (CI 2.1°C, 5.6°C, “true” value 4.1°C) for the experiments based on CGCM3.1(T47), GISS-ER and IPSL-CM4, respectively. However, the three estimates are closer together than the “true” values.

In addition to this experiment, for the CGCM3.1(T47) model, we construct a second training data set with temperature data from 1860 to 2007 and ocean heat content data from 1955 to 2007 (as in the real data). The simulated temperature series acting as the HadCRUT3 series start in 1860, but the two other pairs of “observed” temperatures start here in 1880, to mimic the situation in the real data. The prediction results for this second training period for the CGCM3.1(T47) experiment are shown in Figure 10. In this case, the climate sensitivity is estimated to be 3.5°C (CI 2.4°C, 5.3°C, “true” value 3.4°C).

The predictions and the estimates of the climate sensitivity from our simple model are satisfactory in these two experiments, where both temperature data and ocean heat data are used. However, if we use only the temperature data, the temperature predictions are still very good (not shown), but the climate sensitivity is not estimated well (only for the CGCM3.1(T47) experiment, see Section 3.4 of the Supplementary Material). These results indicate that both the temperatures and the ocean heat content should be used to achieve a robust estimate of the climate sensitivity.

4.3. Test of prediction performance

To test the model’s ability to predict on real data, we re-fit the model by using only data up to and including 1990. This also gives posteriors of the radiative forcings from 1991 to 2007 because each forcing component is strongly correlated in time. With the fitted model, we then predict the hemispheric temperatures and the ocean heat content ahead in time, conditioned on the posteriors of the forcings and the observed SOI index.

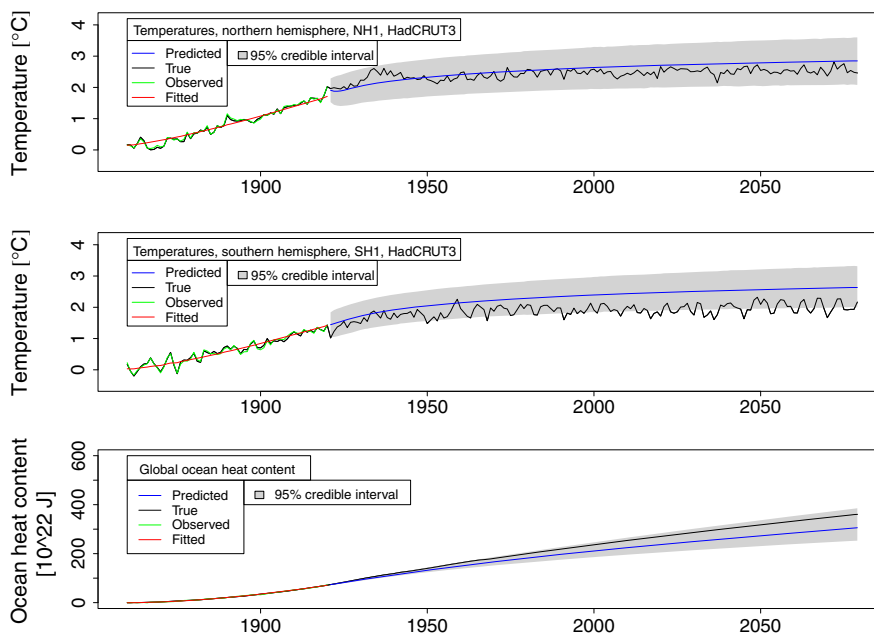


Figure 9. Coupled Model Intercomparison Project phase 3 experiment: True, “observed” and fitted values with corresponding predictions from training data until 1920. For the simulated “observed” temperatures, only the University of East Anglia and the Hadley Centre (HadCRUT3) series are shown, but the Goddard Institute for Space Studies and National Climatic Data Center series are similar

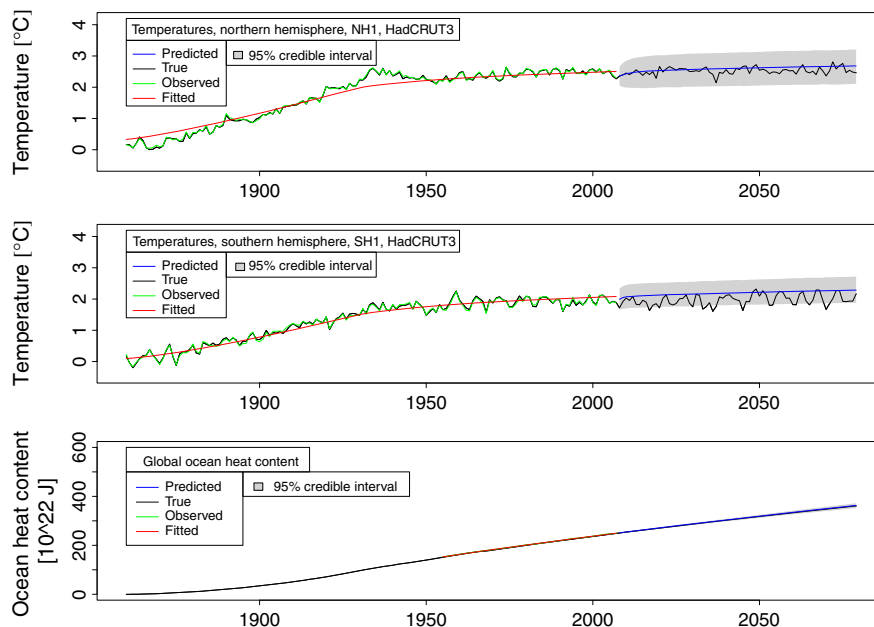


Figure 10. Coupled Model Intercomparison Project phase 3 experiment: True, “observed” and fitted values predictions from training data until 2007. For the simulated “observed” temperatures, only the University of East Anglia and the Hadley Centre (HadCRUT3) series are shown, but the Goddard Institute for Space Studies and National Climatic Data Center series are similar

The predictions with 95% prediction intervals are shown in Figure 11 and can be compared with the observed values in the same period. The model predictions seem to agree reasonably well with the observed values with respect to the given prediction uncertainties.

The corresponding estimate of the climate sensitivity (panel (b), Figure 6) is naturally much more uncertain ($R_{90} = 2.52$) than when all data up to 2007 were used ($R_{90} = 1.17$). We further re-fit the model once more, now using data up to and including 2000 (panel (c), Figure 6). The uncertainty of the climate sensitivity is then smaller ($R_{90} = 1.39$) than when using data up to 1990 but larger than when all data were used, as we could expect.

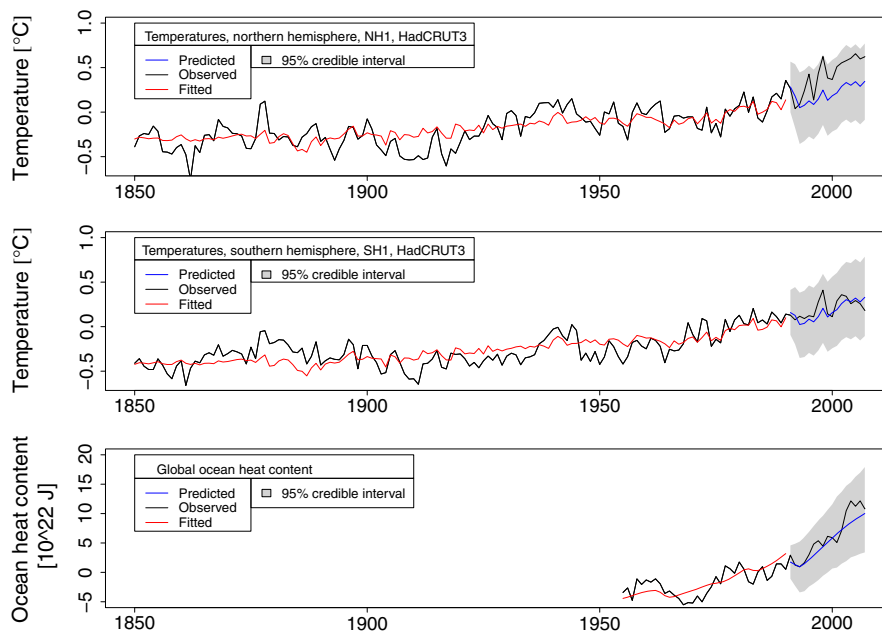


Figure 11. Predictions from 1990 based on a re-fitted model. HadCRUT3, University of East Anglia and the Hadley Centre

4.4. Using other ocean heat content data or averaging the temperatures

So far, we have used the ocean heat content data published by Levitus *et al.* (2009). We now re-fit the model, using each of the two alternative ocean heat content data sets listed in Table 1, see also Figures 1 and 2. The estimate of S is reduced to 1.4°C (CI 0.7°C , 2.7°C) and to 1.7°C (CI 1.0°C , 3.1°C) when the data from Ishii and Kimoto (2009) or Church *et al.* (2011) are used, respectively (see also panels (d) and (e), Figure 6). The estimate of S is rather sensitive to the choice of data source for the ocean heat content, and in the future, it would be sensible to include all three data series in the model simultaneously as for the temperature series.

For the temperatures, we have modelled the three pairs of data series simultaneously. A simpler way to combine them would be to average the three series at each hemisphere and then to use the average temperature series at each hemisphere. Re-fitting this simplified model gives very similar results to using all three series simultaneously (panel (d), Figure 11 of the Supplementary Material). However, we still prefer the simultaneous approach because it implicitly gives the opportunity to down-weight data sources that are not consistent with the rest of the data.

4.5. Sensitivity to the priors of climate model parameters

The priors of the climate model parameters (except the climate sensitivity) were based on our best knowledge from studying existing literature. This involves some subjective choices made by us and depends heavily on the opinions of other scientists. To study how the estimate of the climate sensitivity depends on these choices, we change the original priors to normal priors with unchanged uncertainty and to wider uniform priors. Wider priors give naturally increased uncertainty in the posterior of the climate sensitivity, but the change is not dramatic for priors in a reasonable range (Section 3.5 of the Supplementary Material).

4.6. Uniform prior for the climate feedback parameter $1/S$

So far, we have assumed a rather vague, uniform prior for the climate sensitivity S . However, Frame *et al.* (2005) discussed the role of prior assumptions on S and argued that other priors than uniform could be plausible, depending on the purpose of the analysis. For instance, one could apply a uniform prior for the so-called climate feedback parameter, which is the inverse of S , giving a prior for S that is proportional to $1/S$. To illustrate the role of the prior, we apply this prior on S , but as before, S is restricted to lie between 10^{-4}C and 20°C . This prior is in fact strongly informative towards low climate sensitivities with 76% probability for S being lower than the pure black-body radiation sensitivity of 1.1°C . The resulting posterior (panel (f), Figure 6) is naturally moved towards zero compared with the posterior from the main analysis; however, the posterior probability that S is lower than about 1.1°C is still very small, showing that there is sufficient information in the data to rule out this possibility.

4.7. Sensitivity to the temporal profiles of the temperature standard errors

The temporal profiles of the reported standard errors for the temperatures of the southern hemisphere differ remarkably between HadCRUT3 and NCDC and are also somewhat different at the northern hemisphere. This could be a real difference because they use different methodologies and data sets for estimating the hemispheric temperatures. However, it could also be an artefact because of their different ways of

calculating their uncertainties. Therefore, we compute an alternative temporal profile for each hemisphere as the average of the reported standard errors for HadCRUT3 and NCDC and re-fit the model assuming that HadCRUT3, GISS and NCDC all have these common profiles. This moves the posterior of the climate sensitivity slightly downwards and reduces the uncertainty (panel (g), Figure 6). This is not an obvious result but may be because of a different weighting of old and new temperature data. It can be seen in Figure 2 that newer data will be assigned more weight for HadCRUT3 and less weight for NCDC.

4.8. Adding an extra component to the radiative forcing

So far, nine components have been included in the total radiative forcing. However, other cloud effects such as the cloud lifetime effect (Albrecht, 1989) and the semi-direct effect (Hansen *et al.*, 1997), which are not defined as radiative forcing in a strict sense (Forster *et al.*, 2007; Lohmann *et al.*, 2010), do play a similar role as radiative forcing in our context. The strict definition of radiative forcing used in the IPCC is “the change in net (down minus up) irradiance (solar plus longwave; in W/m^2) at the tropopause after allowing for stratospheric temperatures to readjust to radiative equilibrium, but with surface and tropospheric temperatures and state held fixed at the unperturbed values” (Ramaswamy *et al.*, 2001). The cloud lifetime effect and the semi-direct effect were not included in the IPCC radiative forcing summary (Forster *et al.*, 2007) because the aerosols change the cloud lifetime and hence alter the tropospheric state. But, this change has a rapid response and occurs on a much faster timescale than feedbacks from surface temperature changes. Therefore, in this context, it would be useful to include the cloud lifetime effect. The cloud lifetime effect has until now been set to zero in this study. There are large uncertainties in the value of the cloud lifetime effect (Lohmann and Feichter, 2005), but we have specified two reasonable scenarios on the basis of the interval ($-1.5, -0 W/m^2$) given in the review by Isaksen *et al.* (2009):

- Cloud lifetime effect is proportional to the prior mean of the cloud albedo indirect aerosol component, and its value in 2005 is $-0.25 W/m^2$.
- As earlier, but, the value of the cloud lifetime effect in 2005 is $-0.5 W/m^2$.

The corresponding posteriors of the climate sensitivities are shown in panels (h) and (i) of Figure 6. Including cloud lifetime effect increases the posterior mean of the climate sensitivity with up to $1.3^\circ C$ to a value of about $3.3^\circ C$ and the uncertainty increases as well. An increase in climate sensitivity is expected when the total radiative forcing is reduced (more negative aerosol forcing). The relationship between the total aerosol effect and the climate sensitivity has previously been shown when the observed temperature records are used (Andreae *et al.*, 2005) and in AOGCM simulations of the 20th century where total forcing is inversely correlated with climate sensitivity (Kiehl, 2007). Thus, the estimate from our original analysis should be interpreted with care. In further work, the uncertainty of the cloud lifetime effect should also be taken into account.

4.9. Using an informative prior for the climate sensitivity on the basis of reconstructed temperatures before 1850

Hegerl *et al.* (2006) estimated the climate sensitivity on the basis of reconstructed temperature data from 1505 to 1850. Furthermore, they combined estimates of the climate sensitivity on the basis of observational data (from 1850 or later) from several authors into one probability density function (PDF). Finally, they used the PDF based on observational data as a prior and updated the PDF in a Bayesian way, taking into account their own PDF based on the reconstructed temperatures.

We here do it the other way around. We use the PDF of Hegerl *et al.* (2006) based on the reconstructed temperature data before 1850 (their CH-blend series) as an informative prior, and let all other priors be unchanged compared with our original approach. The resulting estimate of the climate sensitivity is shown in panel (j) of Figure 6. Although the posterior mean is almost the same as that from the main analysis, the uncertainty is naturally less.

Hegerl *et al.* (2006) also calculated a PDF for the climate sensitivity that was a combination of PDFs from several authors but all on the basis of reconstructed temperature data before 1850. We use also this as an informative prior, and the resulting posterior is shown in panel (k) of Figure 6 with a slightly larger uncertainty than in panel (j).

4.10. Information in temperature data versus ocean heat data

To compare the information value of the temperature observations with that of the ocean heat observations, we re-fit the model by using only one of these data sources at time. The resulting estimates of the climate sensitivity are shown in panels (l) and (m) of Figure 6. Using only the temperatures yields slightly less uncertainty than using only the ocean heat content, indicating that the present temperature data are most informative with respect to the climate sensitivity. However, because the data series for the ocean heat content are rather short, this may change in the future. Furthermore, it is reassuring that the posteriors using each of the two data sources alone are similar, as well as both posteriors are consistent with that from the main analysis where the data sources are combined.

5. CONCLUSION

We have presented a method for how the equilibrium climate sensitivity can be estimated from prior estimates of historical radiative forcings and observations of hemispheric temperature changes and ocean heat content, by linking these together with a physically based, deterministic climate model embedded in a data-driven stochastic model. The stochastic part consists of one model error term and another term for observational error.

Our model is very simple compared with the complex climate system it attempts to describe. The simple climate model, which is the core of our full model, does not account for the natural variability in the climate, but the model error \mathbf{n}_t^m is included to account for this. The posterior of the model errors (not shown) indicates multidecadal oscillations, which is a general characteristic of the climate system. The autoregressive process of order one for model errors could therefore perhaps be extended to a second-order process, which can exhibit pseudo-periodic behaviour. However, there are not enough data available to justify such an extension, and we do not expect that this would alter the results significantly. To make probable that our simple model can give a reasonable estimate of the climate sensitivity, the model was validated on simulated data from AOGCMs, on the basis of a much more complex description of the earth's climate, and the results were satisfactory when data for both temperature and ocean heat content were used.

The resulting estimate of the climate sensitivity is slightly smaller than the best estimate given in IPCC (2007) and could be compared with other estimates as well. However, we underscore that our results are sensitive to the indirect aerosol effects, which have a large uncertainty. In this study, the cloud-albedo effect is treated as a radiative forcing mechanism in the main part of the study, whereas other indirect aerosol effects will be parts of the climate feedbacks. Therefore, the estimate of S presented here is likely to be underestimated because the net forcing of the other indirect effects are likely to be negative (Forster *et al.*, 2007). In one of the sensitivity cases, this assumption is further investigated. The results are also influenced by the choice of priors. For instance, using a uniform prior on $1/S$ moves the posterior of S downwards compared with the posterior based on the uniform prior on S . But even if these two priors are very different, they both result in low posterior probabilities for S being less than about 1 or higher than 4, say. The choice of priors will be less important when more data become available.

As mentioned in Section 1, several authors have estimated the climate sensitivity. These estimates are based either on pure physical modelling through AOGCMs, on fitting models to reconstructed temperatures from paleoclimate data, or on fitting models to observed temperatures from industrial time as we did. The approach of Tomassini *et al.* (2009) is the one that is most similar to ours. They used a similar climate model \mathbf{m}_t as ours, included both model errors and observational errors, and fitted their model to both temperature and ocean heat content data, but there are certain differences from our approach. They (i) used only one temperature series; (ii) assumed no autocorrelation in the observational error for temperature; and (iii) did not explicitly model the effect related to the SOI. However, the two most important differences are the following:

- Their model error is handled by an (vector) autoregressive model of order 3 (VAR(3)), which accounts for natural variability, including the SOI-related variability. In our model, this term corresponds to the sum of our model error (VAR(1) and the SOI effect (VAR(2)), which is an autoregressive moving average (VARMA) process of orders 3 and 2 (VARMA(3,2)) (Box and Jenkins, 1970, Section A4.4.2). Their model structure is therefore similar to ours, but Tomassini *et al.* (2009) estimated the model error term from a 900-year long simulation run from an AOGCM under constant forcing. This is an elegant way to account for natural variability, which we want to explore in our future work.
- They do not use informative priors for how far the true radiative forcing can be from their best guess, except that the error are smooth in time. They assume that the true forcing is given by $x_t = \mu_t + \phi_t$, where μ_t is their best guess (prior mean) and ϕ_t is a stochastic, stationary error term that varies smoothly over time but with a variance that is estimated from the data.

We present a few more details of the approach of Tomassini *et al.* (2009) in Section 4 of the Supplementary Material, together with short descriptions of two other estimation methods that are based on observed temperatures.

Our model has been developed to estimate the equilibrium climate sensitivity but may be useful for other purposes as well. For instance, by simulating future temperatures and ocean heat content from the model, it should be possible to quantify how quickly the uncertainty in the equilibrium climate sensitivity estimate will decrease as additional observations become available, similar to what Padilla *et al.* (2011) did for the transient climate sensitivity. Another possibility is to use it for the so-called pattern scaling (e.g. Mitchell, 2003), that is, to create additional, but cheap, scenarios from a computer intensive, complex climate model by scaling the response pattern from one run of the complex model by a global warming projection from a simple climate model. In further work, we intend to improve the equilibrium climate estimate by improving and extending the input data by (i) using data up to at least 2010; (ii) using updated and more precise priors for the forcing components; and (iii) using a prior with uncertainty for the cloud lifetime effect. Another useful extension would be to model several observed ocean heat content series simultaneously.

Acknowledgements

This work was funded by the Research Council of Norway projects ‘‘Constraining total feedback of the climate system by observations and models’’ (184840/S30) and ‘‘Modern Application-driven Statistical Challenges’’ (186951/I30). Ragnar Bang Huseby is acknowledged for the implementation of the Wishart prior (Section 2.4 of the Supplementary Material).

REFERENCES

- Albrecht BA. 1989. Aerosols, cloud microphysics, and fractional cloudiness. *Science* **245**(4923): 1227–1230.
- Ammann CM, Meehl GA, Washington WM, Zender CS. 2003. A monthly and latitudinally varying volcanic forcing dataset in simulations of 20th century climate. *Geophysical Research Letters* **30**. Article Number 1657, 10.1029/2003gl016875.
- Andreae MO, Jones CD, Cox PM. 2005. Strong present-day aerosol cooling implies a hot future. *Nature* **435**(7046): 1187–1190.
- Annan JD, Hargreaves JC. 2011. On the generation and interpretation of probabilistic estimates of climate sensitivity. *Climatic Change* **104**: 423–436. DOI: 10.1007/s10584-009-9715-y.

- Banzon VF, Reynolds RW, Smith TM. 2010. The role of satellite data in the extended reconstruction of sea surface temperatures. In *Oceans from Space*, Barale V, Gower JFR, Alberotanza L (eds): Venice 20201, European Commission, EUR 24324 EN; 27–28. Proceedings.
- Box GEP, Jenkins GM. 1970. Time series analysis: forecasting and control. Holden-Day.
- Brohan P, Kennedy JJ, Harris I, Tett SFB, Jones PD. 2006. Uncertainty estimates in regional and global observed temperature changes: a new dataset from 1850. *Journal of Geophysical Research* **111**. D12106, doi:10.1029/2005JD006548.
- Church J, White N, Konikow L, Domingues C, Cogley J, Rignot E, Gregory J, van den Broeke M, Monaghan A, Velicogna I. 2011. Revisiting the earth's sea-level and energy budgets from 1961 to 2008. *Geophysical Research Letters* **38**, L18601, DOI: 10.1029/2011GL048794.
- Crowley TJ, Baum SK, Kim KY, Hegerl GC, Hyde WT. 2003. Modeling ocean heat content changes during the last millennium. *Geophysical Research Letters* **30**, DOI: 10.1029/2003gl017801. Article Number 1932.
- Domingues C, Church J, White N, Gleckler P, Wijffels S, Barker P, Dunn J. 2008. Improved estimates of upper-ocean warming and multi-decadal sea-level rise. *Nature* **453**: 1090–U6, DOI: 10.1038/nature07080.
- Drignei D, Forest C, Nychka D. 2008. Parameter estimation for computationally intensive nonlinear regression with an application to climate modeling. *The Annals of Applied Statistics* **2**: 1217–1230, DOI: 10.124/08-AOAS210.
- Forest C, Stone P, Sokolov A. 2006. Estimated PDFs of climate system properties including natural and anthropogenic forcings. *Geophysical Research Letters* **33**. L01705, doi:10.129/2005GL023977.
- Forster P, Ramaswamy V, Artaxo P, Bernsten T, Betts R, Fahey DW, Haywood J, Lean J, Lowe DC, Myhre G, Nganga J, Prinn R, Raga G, Schulz M, Dorland RV. 2007. Changes in atmospheric constituents and in radiative forcing. In *Climate Change 2007: The Physical Science Basis. Contribution of Working Group I to the Fourth Assessment Report of the Intergovernmental Panel on Climate Change*, Solomon S, Qin D, Manning M, Chen Z, Marquis M, Averyt KB, Tignor M, Miller HL (eds). Cambridge University Press: Cambridge and New York, NY.
- Frame D, Booth B, Kettleborough J, Stainforth D, Gregory J, Collins M, Allen M. 2005. Constraining climate forecasts: the role of prior assumptions. *Geophysical research letters* **32**.
- Gao CC, Robock A, Ammann C. 2008. Volcanic forcing of climate over the past 1500 years: an improved ice core-based index for climate models. *Journal of Geophysical Research-Atmospheres* **113**. D23111, doi:10.1029/2008jd010239.
- Gregory J, R.J. S, Raper S, Stott P, Rayner N. 2002. An observationally based estimate of the climate sensitivity. *Journal of Climate* **15**: 3117–3121.
- Hansen J, Ruedy R, Sato M, Lo K. 2010. Global surface temperature change. *Reviews of Geophysics* **48**, RG4004, DOI: 10.1029/2010RG000345.
- Hansen J, Sato M. 2011. Paleoclimate implications for human-made climate change. In *Climate Change at the Eve of the Second Decade of the Century: Inferences from Paleoclimate and Regional Aspects: Proceedings of the Milutin Milankovitch 130th Anniversary Symposium*, Berger A, Mesinger F, Šijači D (eds). Springer, in press.
- Hansen J, Sato M, Ruedy R. 1997. Radiative forcing and climate response. *Journal of Geophysical Research* **102**.
- Hegerl G, Crowley T, Hyde W, Frame D. 2006. Climate sensitivity constrained by temperature reconstructions over the past seven centuries. *Nature* **440**, DOI: 10.1038/nature04679.
- Hegerl G, Zwiers F, Braconnot P, Gillett N, Luo Y, Marengo Orsini J, Nicholls N, J.E. P, Stott P. 2007. Understanding and attributing climate change. In *Climate Change 2007: The Physical Science Basis. Contribution of Working Group I to the Fourth Assessment Report of the Intergovernmental Panel on Climate Change*, Solomon S, Qin D, Manning M, Chen Z, Marquis M, Averyt KB, Tignor M, Miller HL (eds). Cambridge University Press: Cambridge and New York, NY.
- Houghton JT, Filho LGM, Callander BA, Harris N, Kattenberg A, Maskell K. 1996. *Climate Change 1995: The Science of Climate Change. Contribution of WGI to the Second Assessment Report of the Intergovernmental Panel of Climate Change*. Cambridge University Press: Cambridge and New York, NY. http://www.ipcc.ch/ipccreports/sar/wg_i/ipcc_sar_wg_i_full_report.pdf.
- Houghton JT, Filho LGM, Griggs DJ, Maskell K. 1997. An introduction to simple climate models used in the IPCC second assessment report, IPCC Technical Paper II. IPCC, Geneva, Switzerland. <http://www.ipcc.ch/pdf/technical-papers/paper-II-en.pdf>.
- Hourdin F, Musat I, Bony S, Braconnot P, Codron F, Dufresne J, Fairhead L, Filiberti M, Friedlingstein P, Grandpeix J, Krinner G, Levan P, Li Z, Lott F. 2006. The LMDZ4 general circulation model: climate performance and sensitivity to parametrized physics with emphasis on tropical convection. *Climate Dynamics* **27**: 787–813, DOI: 10.1007/s00382-006-0158-0.
- IPCC. 2007. *The Physical Science Basis. Contribution of Working Group I to the Fourth Assessment Report of the Intergovernmental Panel on Climate Change*. Cambridge University Press: Cambridge and New York, NY. http://www.ipcc.ch/publications_and_data/publications_ipcc_fourth_assessment_report_wg1_report_the_physical_science_basis.htm.
- Isaksen I, Granier C, Myhre G, Bernsten T, Dalsoren S, Gauss M, Klimont Z, Benestad R, Bousquet P, Collins W, Cox T, Eyring V, Fowler D, Fuzzi S, Jockel P, Laj P, Lohmann U, Maione M, Monks P, Prevo A, Raes F, Richter A, Rognerud B, Schulz M, Shindell D, Stevenson D, Storelmo T, Wang W, van Weele M, Wild M, Wuebbles D. 2009. Atmospheric composition change: climate-chemistry interactions. *Atmospheric Environment* **43**: 5138–5192, DOI: 10.1016/j.atmosenv.2009.08.003.
- Ishii M, Kimoto M. 2009. Reevaluation of historical ocean heat content variations with time-varying XBT and MBT depth bias corrections. *Journal of Oceanography* **65**, DOI: 10.1007/s10872-009-0027-7.
- Kennedy M, O'Hagan A. 2001. Bayesian calibration of computer models. *Journal of the Royal Statistical Society Series B* **63**: 425–450.
- Kiehl JT. 2007. Twentieth century climate model response and climate sensitivity. *Geophysical Research Letters* **34**.
- Knight J, Allan R, Folland C, Vellinga M, Mann M. 2005. A signature of persistent natural thermohaline circulation cycles in observed climate. *Geophysical Research Letters* **32**. L20708, doi:10.1029/2005GL024233.
- Knutti R, Hegerl GC. 2008. The equilibrium sensitivity of the earth's temperature to radiation changes. *Nature Geoscience* **1**(11): 735–743.
- Künsch H. 1989. The jackknife and the bootstrap for general stationary observations. *The Annals of Statistics* **17**: 1217–1261.
- Levitus S, Antonov JI, Boyer TP, Locarnini RA, Garcia HE, Mishonov AV. 2009. Global ocean heat content 1955–2008 in light of recently revealed instrumentation problems. *Geophysical Research Letters* **36**. L07608, doi:10.1029/2008GL037155.
- Lohmann U, Feichter J. 2005. Global indirect aerosol effects: a review. *Atmospheric Chemistry and Physics* **5**: 715–737.
- Lohmann U, Rotstain L, Storelmo T, Jones A, Menon S, Quaas J, Ekman A, Koch D, Ruedy R. 2010. Total aerosol effect: radiative forcing or radiative flux perturbation?. *Atmospheric Chemistry and Physics* **10**: 3235–3246.
- Meehl GA, Washington WM, Ammann CM, Arblaster JM, Wigley TML, Tebaldi C. 2004. Combinations of natural and anthropogenic forcings in twentieth-century climate. *Journal of Climate* **17**: 3721–3727.
- Mitchell T. 2003. Pattern scaling: an examination of the accuracy of the technique for describing future climates. *Climatic Change* **60**: 217–242, DOI: 10.1023/A:1026035305597.
- Myhre G, Myhre A, Stordal F. 2001. Historical evolution of radiative forcing of climate. *Atmospheric Environment* **35**: 2361–2373.
- Olivie D, Stuber N. 2010. Emulating AOGCM results using simple climate models. *Climate Dynamics* **35**: 1257–1287.
- Padilla L, Vallis G, Rowley C. 2011. Probabilistic estimates of transient climate sensitivity subject to uncertainty in forcing and natural variability. *Journal of Climate*: To appear, DOI: 10.1175/2011JCLI3989.1, (to appear in print).
- Ramaswamy V, Boucher O, Haigh J, Hauglustaine D, Haywood J, Myhre G, Nakajima T, Shi G, Solomon SR. 2001. Radiative forcing of climate change. In *Climate Change 2001: The Physical Science Basis. Contribution of Working Group I to the Third Assessment Report of the Intergovernmental Panel*

- on *Climate Change*, J.T. Houghton J, Ding Y, Griggs D, Noguer M, van der Linden P, Dai X, Maskell K, Johnson C (eds). Cambridge University Press: Cambridge and New York, NY.
- Randall D, Wood R, Bony S, Colman R, Fichetef T, Fyfe J, Kattsov V, Pitman A, Shukla J, Srinivasan J, Stouffer R, Sumi A, Taylor K. 2007. Climate models and their evaluation. In *Climate Change 2007: The Physical Science Basis. Contribution of Working Group I to the Fourth Assessment Report of the Intergovernmental Panel on Climate Change*, Solomon S, Qin D, Manning M, Chen Z, Marquis M, Averyt KB, Tignor M, Miller HL (eds). Cambridge University Press: Cambridge and New York, NY.
- Roe GH, Baker MB. 2007. Why is climate sensitivity so unpredictable?. *Science* **318**(5850): 629–632.
- Sansó B, Forest C. 2009. Statistical calibration of climate system properties. *Journal of the Royal Statistical Society Series C – Applied Statistics* **58**: 485–503.
- Sato M, Hansen JE, McCormick MP, Pollack JB. 1993. Stratospheric aerosol optical depths 1850–1990. *Journal of Geophysical Research-Atmospheres* **98**: 22987–22994.
- Schlesinger ME, Jiang X, Charlson RJ. 1992. Implication of anthropogenic atmospheric sulphate for the sensitivity of the climate system. In *Climate Change and Energy Policy: Proceedings of the International Conference on Global Climate Change: Its Mitigation Through Improved Production and Use of Energy*, Rosen L, Glasser R (eds). Los Alamos National Laboratory, New Mexico; 75–108. Proceedings.
- Schmidt G, Ruedy R, Hansen J, Aleinoy I, Bell N, Bauer M, Bauer S, Cairns B, Canuto V, Cheng Y, Del Genio A, Faluvegi G, Friend A, Hall T, Hu Y, Kelley M, Kiang N, Koch D, Lacis A, Lerner J, Lo K, Miller R, Nazarenko L, Oinas V, Perlwitz J, Perlwitz J, Rind D, Romanou A, Russell G, Sato M, Shindell D, Stone P, Sun S, Tausnev N, Thresher D, Yao M. 2006. Present-day atmospheric simulations using giss modele: comparison to in situ, satellite, and reanalysis data. *Journal of Climate* **19**: 153–192, DOI: 10.1175/JCLI3612.1.
- Scinocca JF, McFarlane NA, Lazare M, Li J, Plummer D. 2008. Technical note: the CCCMA third generation AGCM and its extension into the middle atmosphere. *Atmospheric Chemistry and Physics* **8**: 7055–7074, DOI: 10.5194/acp-8-7055-2008.
- Semenov V, Latif M, Dommengot D, Keenlyside N, Strehz A, Martin T, Wonsun P. 2010. The impact of north atlantic-arctic multidecadal variability on northern hemisphere surface air temperature. *Journal of Climate* **23**: 5668–5677.
- Skeie R, Fuglestedt J, Berntsen T, Lund M, Myhre G, Rypdal K. 2009. Global temperature change from the transport sectors: historical development and future scenarios. *Atmospheric Environment* **43**: 6260–6270, DOI: 10.1016/j.atmosenv.2009.05.025.
- Smith TM, Reynolds RW. 2005. A global merged land air and sea surface temperature reconstruction based on historical observations (1880–1997). *Journal of Climate* **18**: 2021–2036.
- Smith TM, Reynolds RW, Peterson TC, Lawrimore J. 2008. Improvements to NOAA's historical merged land-ocean surface temperature analysis (1880–2006). *Journal of Climate* **21**: 2283–2296.
- Soden BJ, Held IM. 2006. An assessment of climate feedbacks in coupled ocean-atmosphere models. *Journal of Climate* **19**(14): 3354–3360.
- Stainforth DA, Aina T, Christensen C, Collins M, Faull N, Frame D, Kettleborough J, Knight S, Martin A, Murphy J, Piani C, Sexton D, Smith L, Spicer R, Thorpe A, Allen M. 2005. Uncertainty in predictions of the climate response to rising levels of greenhouse gases. *Nature* **433**: 403–406.
- Tomassini L, Reichert P, Künsch H, Buser C, Knutti R. 2009. A smoothing algorithm for estimating stochastic, continuous-time model parameters and its application to a simple climate model. *Journal of the Royal Statistical Society Series C – Applied Statistics* **58**: 679–704.
- Trenberth K, Jones P, Ambenje P, Bojariu R, Easterling D, Klein Tank A, Parker D, Rahimzadeh F, Renwick J, Rusticucci M, B. S, Zhai P. 2007. Observations: surface and atmospheric climate change. In *Climate Change 2007: The Physical Science Basis. Contribution of Working Group I to the Fourth Assessment Report of the Intergovernmental Panel on Climate Change*, Solomon S, Qin D, Manning M, Chen Z, Marquis M, Averyt KB, Tignor M, Miller HL (eds). Cambridge University Press: Cambridge and New York, NY.
- Trenberth KE, Caron JM, Stepaniak DP, Worley S. 2002. Evolution of El Niño–Southern Oscillation and global atmospheric surface temperatures. *Geophysical research letters* **107**. 4065, doi:10.1029/2000jd000298.
- urlCMIP3. Cmp3 data. http://www-pcmdi.llnl.gov/ipcc/about_ipcc.php, Program for Climate Model Diagnosis and Comparisons, USA.
- urlCSIRO. CSIRO ocean heat content data. http://www.cmar.csiro.au/sealevel/sl_data_cmar.html [accessed 15. October 2011], Commonwealth Scientific and Industrial Research Organisation, Australia.
- urlGISS. Giss temperature data for the northern and southern hemispheres. <http://data.giss.nasa.gov/gistemp/tabledata/NH.Ts+dSST.txt> and <http://data.giss.nasa.gov/gistemp/tabledata/SH.Ts+dSST.txt> [accessed 12. May 2010], Goddard Institute for Space Studies, USA.
- urlHadCRUT3. Hadcrut3 temperature data for the northern and southern hemispheres. <http://hadobs.metoffice.com/hadcrut3/diagnostics/hemispheric/northern/annual> and <http://hadobs.metoffice.com/hadcrut3/diagnostics/hemispheric/southern/annual> [accessed 18. May 2010], Hadley Centre, UK.
- urlNCDC. NCDC temperature data. ftp://ftp.ncdc.noaa.gov/pub/data/cmb/mlost/pdo/aravg.ann.land_ocean.00N.90N.asc and ftp://ftp.ncdc.noaa.gov/pub/data/cmb/mlost/pdo/aravg.ann.land_ocean.00S.90S.asc, National Climatic Data Center, USA.
- urlNODC. Levitus ocean heat content data. ftp://ftp.nodc.noaa.gov/pub/data.nodc/woa/DATA_ANALYSIS/3M_HEAT_CONTENT/DATA/basin/yearly/h22-w0-700m.dat [accessed 20. May 2010], updated later in September 2010, see ftp://ftp.nodc.noaa.gov/pub/data.nodc/woa/DATA_ANALYSIS/3M_HEAT_CONTENT/PDF/heat_content_differences.pdf, National Oceanographic Data Center, USA.
- urlSOI. Southern Oscillation Index data. <http://www.bom.gov.au/climate/current/soihtm1.shtml> [accessed May 2010], Bureau of Meteorology, Australia.